

Electrochemical Detection of Daphnetin Based on a Glassy Carbon Electrode Modified with Nafion and RGO-TEPA

Ming Zhou, Yunjie Sheng, Yangchun Li, Yurong Wang*

College of Pharmaceutical Science, Zhejiang Chinese Medical University, Hangzhou 310053, China

*E-mail: wangyr@zcmu.edu.cn

Received: 2 December 2020 / Accepted: 25 January 2021 / Published: 28 February 2021

A sensitive electrochemical sensor composed of Nafion, tetraethylene pentamine-functionalized reduced graphene oxide (RGO-TEPA), and a glassy carbon electrode (GCE) was developed to analyze daphnetin (DAPH). The electrochemical behavior of DAPH on Nafion/RGO-TEPA/GCE was studied by cyclic voltammetry. The electroanalytical method for DAPH detection was established using differential pulse voltammetry. A detection limit of 0.5 nM ($S/N = 3$) and a linear calibration range of 0.1 to 10 μM were obtained. The reproducibility and repeatability of the method were calculated to be 1.6% and 4.8%, respectively. The sensor showed good selectivity for DAPH and was successfully applied to detect DAPH in Zushima tablets. The content of DAPH in Zushima tablets detected by our sensor agreed well with that detected by HPLC.

Keywords: Daphnetin; electrochemical sensor; Nafion; reduced graphene oxide-tetraethylene pentamine (RGO-TEPA)

1. INTRODUCTION

Coumarin frameworks are ubiquitous in various medicinal compounds and play a crucial role in pharmaceuticals [1]. In particular, daphnetin (7,8-dihydroxycoumarin, DAPH) is one of the most important coumarin derivatives because of its multiple pharmacological effects and broad clinical applications [2–5]. For example, DAPH was found to be one of the major active ingredients in the Chinese medicinal herb Zushima, which is widely used to treat coagulation disorders and rheumatoid arthritis in China [6]. Due to its importance, the development of convenient, sensitive, and inexpensive methods for DAPH content detection is a meaningful task for quality control in pharmaceuticals. Traditionally, liquid chromatography (LC) and high-performance liquid chromatography (HPLC) are applied for the detection of DAPH content [7,8]. However, these methods have major drawbacks, namely, they are relatively time-consuming, require expensive equipment, and use of toxic solvents. Alternatively, electrochemical approaches have been used to detect the DAPH content in pharmaceutical

formulations with good detection sensitivity and a reasonable detection limit [9]. Furthermore, it has been demonstrated that nanocomposite-modified electrodes can sensitively increase the electrochemical response to DAPH [10,11].

In the last decade, reduced graphene oxide (RGO) has been increasingly studied for fabricating electrochemical sensors or biosensors because of its excellent electrochemical properties and large surface area [12,13]. Reduced graphene oxide-tetraethylene pentaamine (RGO-TEPA), a novel combination of RGO and TEPA by C-N covalent bonding, has been developed as an excellent substrate material for the modification of electrochemical immunosensors to detect numerous target analytes, such as monocyte chemoattractant protein-1 [14], fibroblast growth factor receptor 3 gene [15], T-2 toxin [16], and several cancer markers [17–22]. It has been found that the existence of the large number of amino groups in RGO-TEPA not only improves the stability of RGO but also allows the material to be modified by metals.

In this study, we develop a sensitive electrochemical method for the detection of DAPH based on using an RGO-TEPA-modified glassy carbon electrode (GCE) as a novel electrochemical sensor. To the best of our knowledge, this is the first attempt to use an RGO-TEPA-modified electrochemical sensor to sensitively increase the electrochemical response of a pharmaceutical formulation.

2. EXPERIMENTAL

2.1 Reagents and instruments

A standard DAPH reagent (98%) was purchased from Shanghai Yuanye Bio-Technology Co., Ltd. (Shanghai, China). RGO and RGO-TEPA were provided by Nanjing/Jiangsu XFNANO Materials Tech Co., Ltd. (Nanjing, China). A 5% Nafion solution was received from Sigma-Aldrich (St. Louis, Missouri, USA). The standard DAPH stock solution (1 mM) was prepared with anhydrous methanol and stored at 4°C in the dark. The supporting electrolyte (a 0.1 M phosphate buffered saline (PBS) solution) was prepared by mixing NaH_2PO_4 and Na_2HPO_4 solutions. The low pH value of PBS was adjusted with 0.1 M H_3PO_4 solution. Working standards were prepared daily by diluting the stock solution to the desired concentration with PBS. All the other chemicals were of analytical grade or better and used as received. All the water used in this work was obtained from a Smart-DUVF water purification system (Shanghai Hitech Instruments Co., Ltd., China) with an electrical resistance of 18.2 M Ω cm.

Cyclic voltammetry (CV) and differential pulse voltammetry (DPV) were conducted with a CHI660 electrochemical workstation (Shanghai Chenhua Instrument Co., Ltd., Shanghai, China). Electrochemical impedance spectroscopy (EIS) was carried out on an RST5210F electrochemical workstation (Suzhou Risetest Electronic Co., Ltd., Suzhou, China). A conventional three-electrode system was applied in the experiment with a bare or modified glassy carbon electrode (GCE, 3 mm diameter) as the working electrode and Ag/AgCl and platinum wire as the reference and counter electrodes, respectively. A PHS-3E pH meter (China Shanghai Electric Instrument Co., Ltd., China) was used for pH adjustments.

2.2 Preparation of the modified electrodes

Before modification, the bare GCE was mechanically polished to a mirror-like surface in turn with abrasive paper and 0.3 and 0.05 μm alumina slurries. Then, the samples were cleaned ultrasonically in ethanol and ultrapure water for 5 min each. Finally, the samples were dried in air at room temperature.

The purchased RGO-TEPA powder was ultrasonically dispersed in ultrapure water for 1 h to obtain a 1.0 mg mL^{-1} homogenous dispersion. Before coating with Nafion, a 0.5 wt.% Nafion solution was prepared by diluting a 5 wt.% Nafion solution in absolute ethanol (≥ 99.7 wt.%). Next, RGO-TEPA/GCE was obtained by carefully casting an 8 μL RGO-TEPA suspension on the electrode surface and drying under an infrared lamp. Nafion/RGO-TEPA/GCE was obtained by dropwise adding 2 μL of 0.5% Nafion ethanol solution onto the surface of dried RGO-TEPA/GCE. Thus, the Nafion/RGO-TEPA/GCE sensor was developed layer by layer.

2.3 Real sample solution preparation

Zushima tablets were purchased from a local pharmacy in Hangzhou. Tablet powder was obtained from finely powdering 10 Zushima tablets in an agate mortar. The accurately weighed powder (0.3610 g) was transferred into 50 mL of 85% methanol and dissolved by ultrasonication for 30 min to obtain a homogenized suspension. The supernatant was collected by centrifugation and filtration. The sample solution was stored at 4 $^{\circ}\text{C}$ in the dark. Before each measurement, a certain amount of sample was diluted to 10 mL with 0.1 M PBS (pH = 2.2).

3. RESULTS AND DISCUSSION

3.1 Electrochemical behaviors of Nafion/RGO-TEPA/GCE

The electron transfer ability of the redox reaction on the Nafion/RGO-TEPA/GCE surface was verified by EIS using a 5 mM $\text{K}_3\text{Fe}(\text{CN})_6/\text{K}_4\text{Fe}(\text{CN})_6$ solution (containing 0.1 M KCl) as an electrochemical probe with an applied frequency range from 0.01 Hz to 1 MHz and an amplitude of 5 mV. The bare GCE, RGO/GCE, RGO-TEPA/GCE, and Nafion/RGO/GCE were also detected for comparison, and the obtained results were reported in the form of Nyquist plots (Fig. 1).

In the EIS curve, the diameter of the semicircle is equal to the Randles circuit (R_{ct}) value which is related to the electron transfer kinetics of the redox probe at the electrode/electrolyte interface. The R_{ct} values of the bare GCE, RGO/GCE, RGO-TEPA/GCE, Nafion/RGO/GCE, and Nafion/RGO-TEPA/GCE were calculated to be approximately 149, 66, 60, 55, and 43 Ω , respectively. These results demonstrated that Nafion/RGO-TEPA accelerated the electron transfer between the electrode surface and the electrochemical probe $\text{K}_3\text{Fe}(\text{CN})_6/\text{K}_4\text{Fe}(\text{CN})_6$.

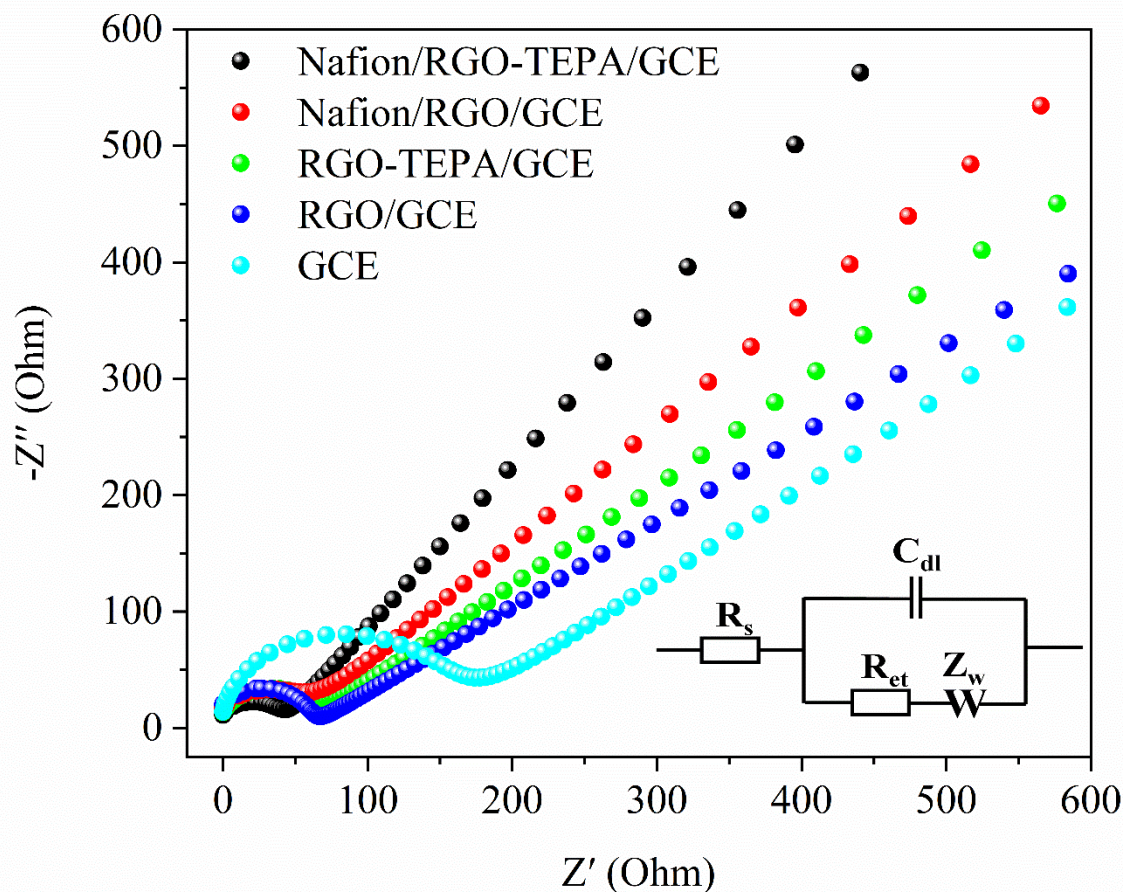


Figure 1. EIS of the bare GCE, RGO/GCE, RGO-TEPA/GCE, Nafion/RGO/GCE, and Nafion/RGO-TEPA/GCE in 5.0 mM $K_3Fe(CN)_6/K_4Fe(CN)_6$ solution containing 0.1 M KCl.

The active area of an electrode can be estimated by chronocoulometry. Fig. 2A shows the single-potential-step chronocoulometric curves of the bare GCE, RGO/GCE, RGO-TEPA/GCE, Nafion/RGO/GCE, and Nafion/RGO-TEPA/GCE in a 1 mM $K_3Fe(CN)_6$ solution containing 0.1 M KCl. The corresponding $Q-t^{1/2}$ plots are provided in Fig. 2B, and the linear relationships of $Q-t^{1/2}$ were expressed as Q (μC) = 14.4694 $t^{1/2}$ + 0.6694 ($R^2 = 0.9996$), Q (μC) = 21.9014 $t^{1/2}$ + 1.2621 ($R^2 = 0.9923$), Q (μC) = 28.6747 $t^{1/2}$ + 4.2133 ($R^2 = 0.9942$), Q (μC) = 50.4908 $t^{1/2}$ + 3.9289 ($R^2 = 0.9977$) and Q (μC) = 60.2945 $t^{1/2}$ + 7.8804 ($R^2 = 0.9904$), for the bare GCE, RGO/GCE, RGO-TEPA/GCE, Nafion/RGO/GCE, and Nafion/RGO-TEPA/GCE, respectively. According to the Anson equation (1) [23],

$$Q = \frac{2nFAC(Dt)^{1/2}}{\pi^{1/2}} + Q_{dl} + Q_{ads} \quad (1)$$

where Q_{dl} is the double-layer charge, Q_{ads} is the Faraday charge, F is the Faraday constant, A (cm^2) is the active area of the working electrode, c ($mol \cdot cm^{-3}$) is the concentration of the substrate, n is the number of electrons transferred and D ($cm^2 \cdot s^{-1}$) is the diffusion coefficient, the value of n was 1 and D was $7.6 \times 10^{-6} cm^2 \cdot s^{-1}$ in the $K_3Fe(CN)_6$ solution [24].

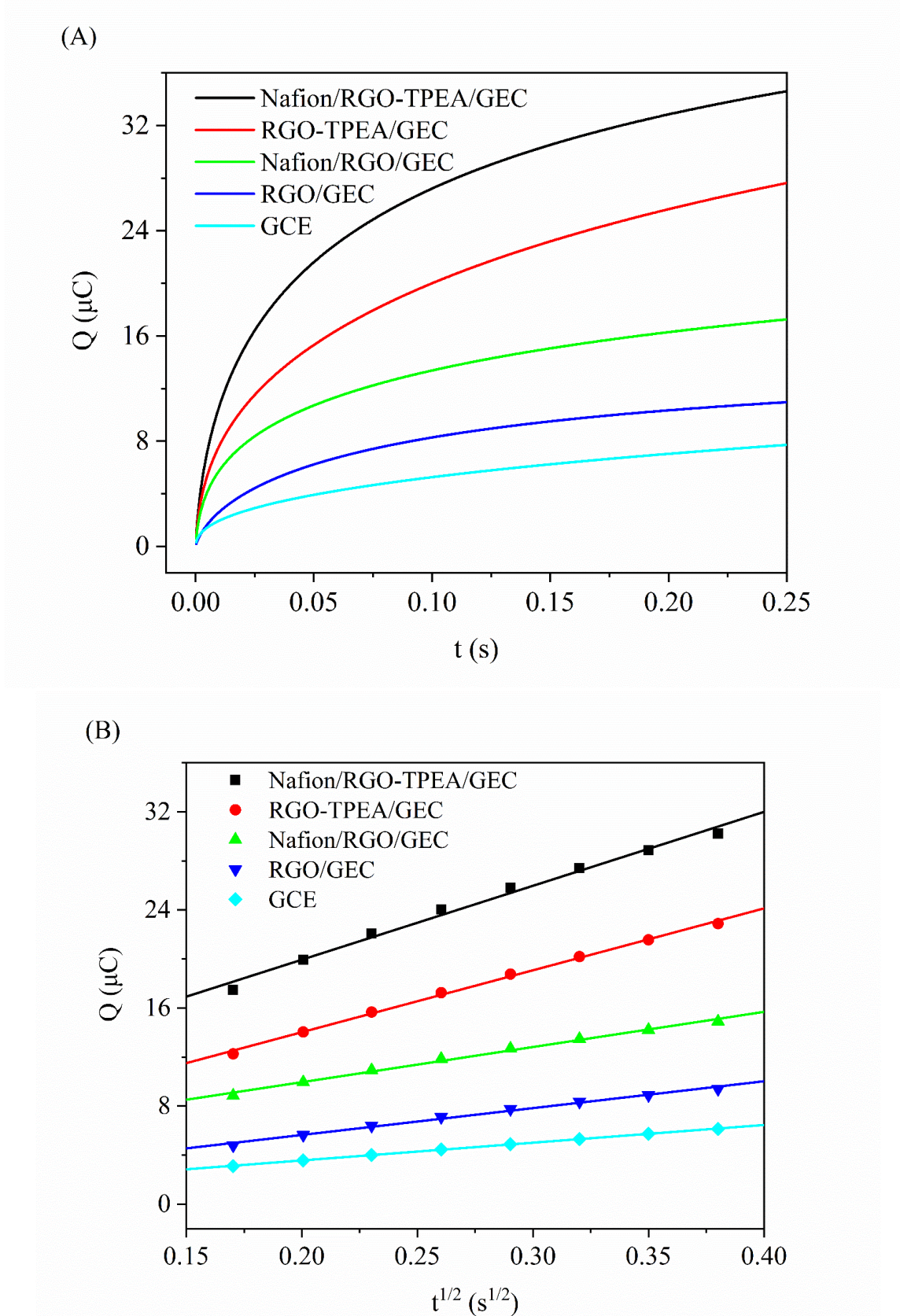


Figure 2. (A) Chronocoulometric curves of the bare GCE, RGO/GCE, RGO-TEPA/GCE, Nafion/RGO/GCE, and Nafion/RGO-TEPA/GCE in a 1 mM $\text{K}_3\text{Fe}(\text{CN})_6$ solution containing 0.1 M KCl. (B) The corresponding $Q-t^{1/2}$ plots.

From the slope value of the regression equation of $Q-t^{1/2}$, the active areas of the above electrodes were calculated to be 0.048 cm^2 , 0.073 cm^2 , 0.096 cm^2 , 0.168 cm^2 and 0.201 cm^2 . These results indicated that the active area of Nafion/RGO-TEPA/GCE was approximately 4 times that of the bare GCE and much larger than that of the other electrodes. This large active area was beneficial for providing more electroactive sites to increase the electrochemical response of DAPH on Nafion/RGO-TEPA/GCE.

3.2 Electrochemical behavior of DAPH on the Nafion/RGO-TEPA/GCE

The electrochemical behaviors of DAPH on the bare GCE, RGO/GCE, RGO-TEPA/GCE, Nafion/RGO/GCE, and Nafion/RGO-TEPA/GCE were investigated by CV. As shown in Fig. 3, an enhanced redox current peak of DAPH with the largest background current was obtained on the Nafion/RGO-TEPA/GCE sensor compared with that of the RGO-TEPA/GCE, Nafion/RGO/GCE, RGO/GCE, and bare GCE sensors. The highest peak current observed might be due to the fast electron transfer kinetics on the Nafion/RGO-TEPA/GCE-modified electrode and the hydrogen bond formed between the amino groups in TEPA and the carbonyl groups in DAPH. The largest background current of the Nafion/RGO-TEPA/GCE might be due to the large effective surface area of the electrode. Therefore, it is feasible to detect DAPH with Nafion/RGO-TEPA/GCE.

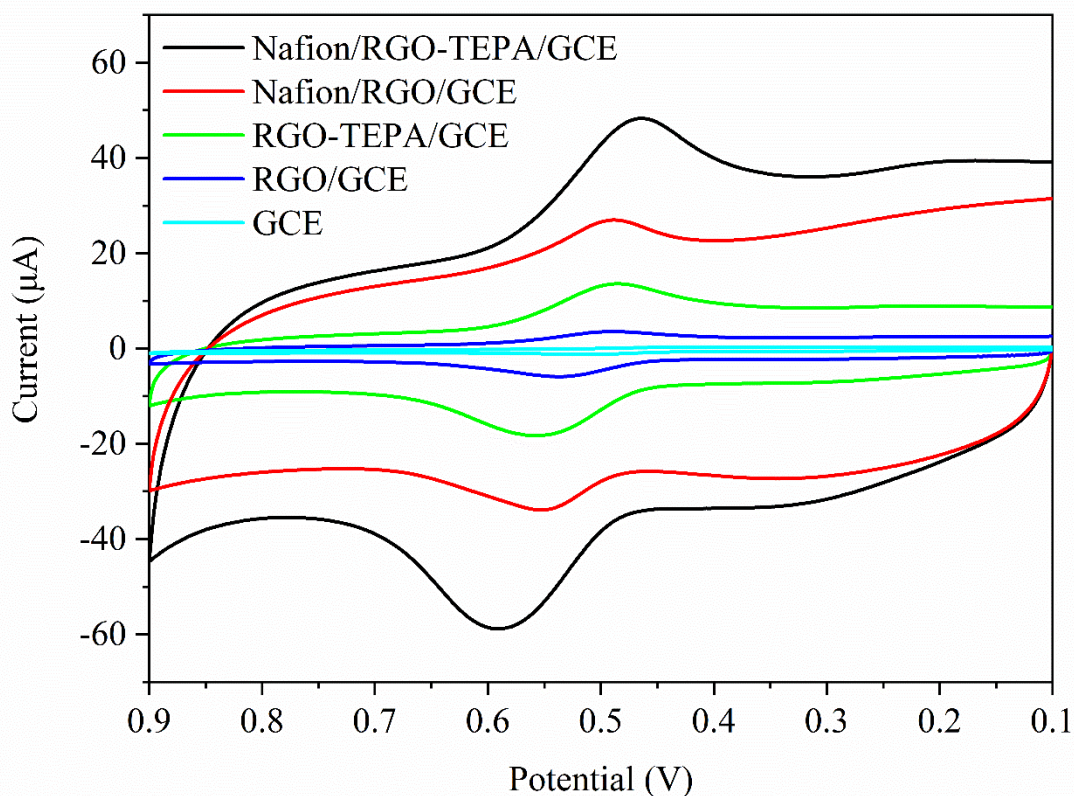
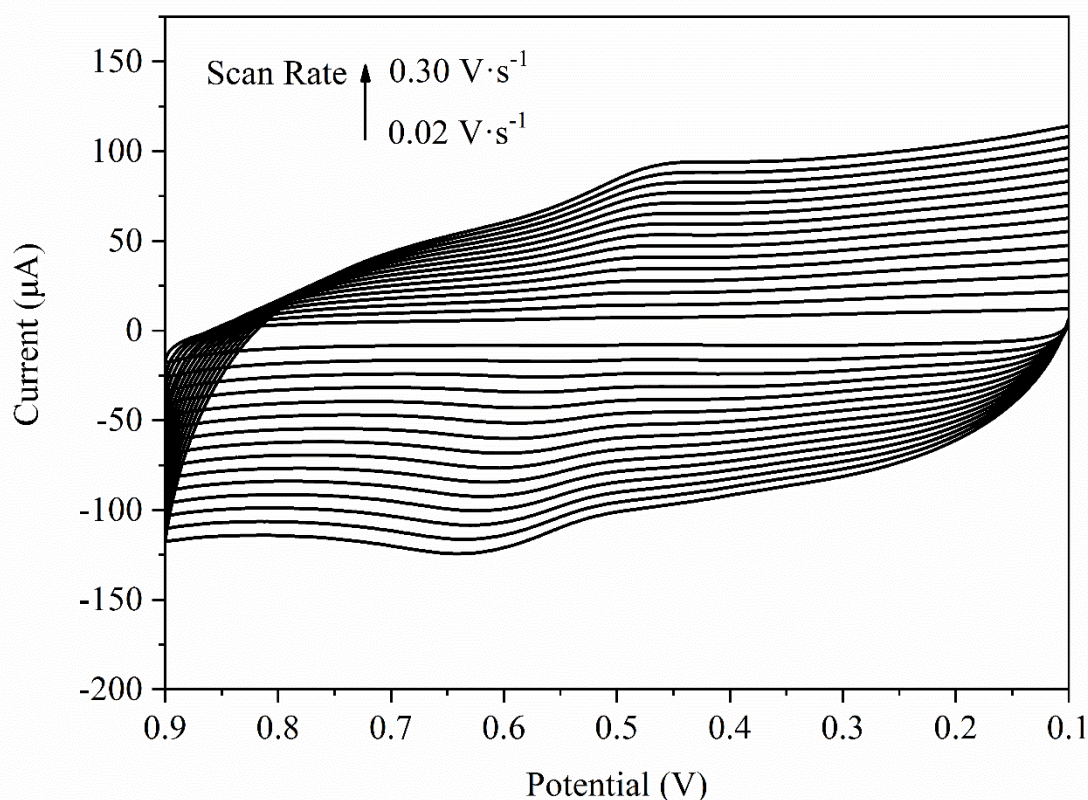


Figure 3. CV curves of DAPH ($10 \mu\text{M}$) on the bare GCE, RGO/GCE, Nafion/RGO/GCE, RGO-TEPA/GCE, and Nafion/RGO-TEPA/GCE sensors in 0.1 M PBS ($\text{pH} = 2.2$) containing $10 \mu\text{M}$ DAPH at a scan rate of $50 \text{ mV}\cdot\text{s}^{-1}$.

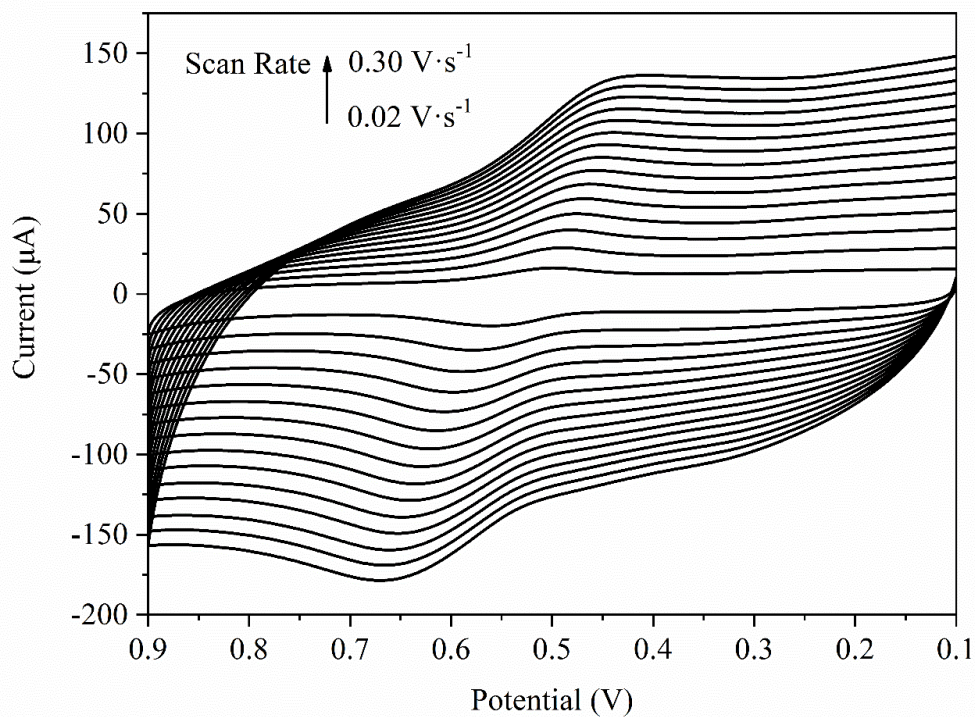
3.3 Effect of the scan rate

The electrochemical responses of DAPH (10 μM) at different scan rates before and after accumulation were investigated by CV to discuss the redox mechanism (Fig. 4). As shown in Fig. 4A-D, the redox peak currents increased with the scan rate from 0.02 to 0.3 V s^{-1} . Moreover, after DAPH accumulated, the redox peak currents were greater than those before accumulation. Fig. 4C shows, that both the oxidation peak current (I_{pa}) and the reduction peak current (I_{pc}) have a good linear range with the scan rate (ν). The fitting linear regression equations are as follows: $I_{\text{pa}} (\mu\text{A}) = -67.10\nu (\text{V}\cdot\text{s}^{-1}) + 2.15$ ($R^2 = 0.9939$) and $I_{\text{pc}} (\mu\text{A}) = 56.35\nu (\text{V}\cdot\text{s}^{-1}) - 1.51$ ($R^2 = 0.9956$), indicating that the electrochemical process of DAPH on Nafion/RGO-TEPA/GCE before accumulation is an adsorption-controlled process. Additionally, Fig. 4D shows, that I_{pa} and I_{pc} have a good linear range with the square root of the scan rate ($\nu^{1/2}$). The fitting linear regression equations can be expressed as follows: $I_{\text{pa}} (\mu\text{A}) = -75.89\nu^{1/2} (\text{V}^{1/2}\cdot\text{s}^{-1/2}) + 3.73$ ($R^2 = 0.9980$) and $I_{\text{pc}} (\mu\text{A}) = 65.53\nu^{1/2} (\text{V}^{1/2}\cdot\text{s}^{-1/2}) - 2.87$ ($R^2 = 0.9984$), indicating that the electrochemical process of DAPH on Nafion/RGO-TEPA/GCE after accumulation is a diffusion-controlled process.

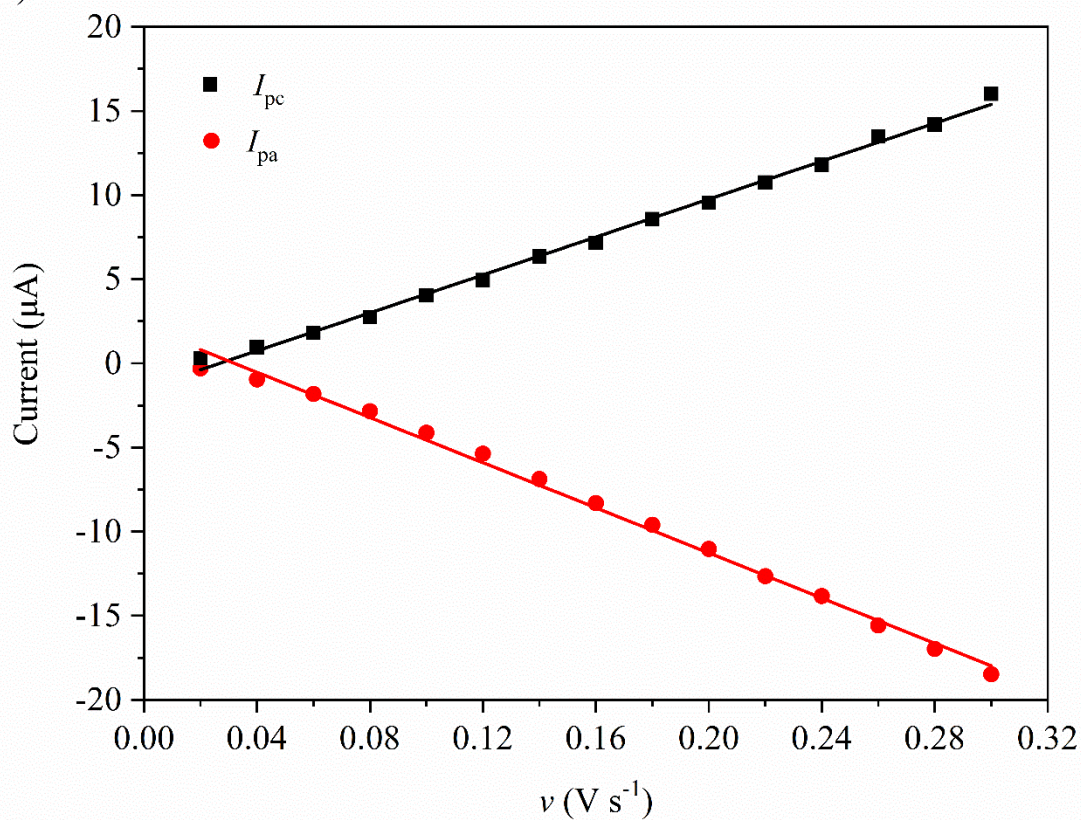
(A)



(B)



(C)



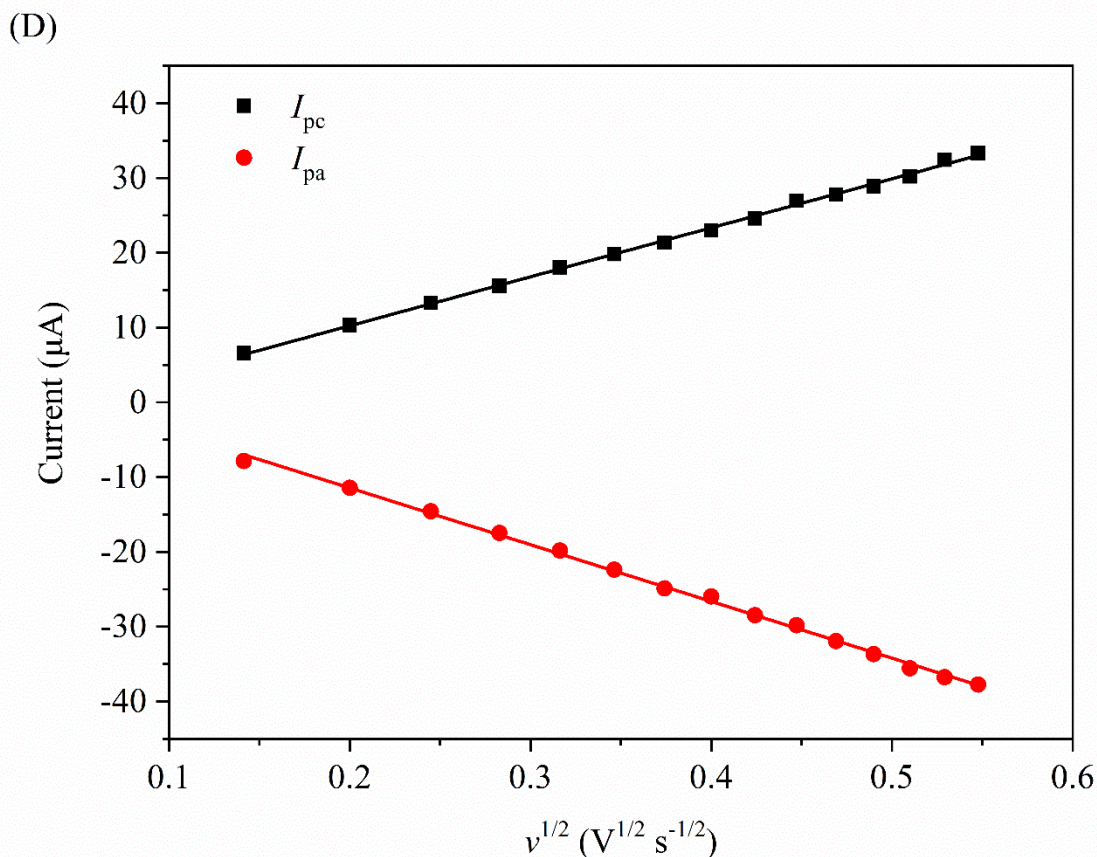


Figure 4. CV curves of DAPH (10 μ M) on Nafion/RGO-TEPA/GCE in 0.1 M PBS (pH = 2.2) at different scan rates from 0.02 to 0.30 $V \cdot s^{-1}$ with 20 $mV s^{-1}$ intervals before (A) and after (B) accumulation. (C) Linear relationship obtained for the redox peak current vs. the scan rate. (D) Linear relationship obtained for the redox peak current vs. the square root of the scan rate.

The relationship between the scan rate and redox peak potential (E) was deduced from Fig. 4A and is shown in Fig. 5. With an increasing scan rate, the oxidation peak potential (E_{pa}) positively shifted, and the reduction peak potential (E_{pc}) negatively shifted, indicating a quasi-reversible electrode process. For the model of a surface-controlled process, the electron transfer kinetics of daphnetin on Nafion/RGO-TEPA/GCE could be deduced by the Laviron equations (2-4) [25]:

$$E_{pa} = E^{0'} + \frac{RT}{(1-\alpha)nF} \ln v \quad (2)$$

$$E_{pc} = E^{0'} - \frac{RT}{\alpha nF} \ln v \quad (3)$$

$$\lg k_s = \alpha \lg(1-\alpha) + (1-\alpha) \lg \alpha - \lg \frac{RT}{nFv} - \alpha(1-\alpha) \frac{nF\Delta E_p}{2.303RT} \quad (4)$$

where, $E^{0'}$ is the formal standard potential, k_s is the apparent heterogeneous electron transfer rate constant, n is the electron transfer number, α is the charge transfer coefficient, v is the scan rate, and ΔE_p is the peak-to-peak potential separation.

When $v > 0.06 V \cdot s^{-1}$, E_{pa} and E_{pc} had a good linear relationship with $\ln v$ providing regression equations of E_{pa} (V) = 0.0418 $\ln v$ + 0.6794 ($R^2 = 0.9868$) and E_{pc} (V) = -0.0231 $\ln v$ + 0.4428 ($R^2 =$

0.9852). Based on the slopes of the E_{pa} - $\ln v$ and E_{pc} - $\ln v$ lines, n and α were calculated to be 1.7 and 0.64, respectively. Since n should be an integer, there were 2 electrons involved in the redox reaction of DAPH at Nafion/RGO-TEPA/GCE. Additionally, according to equation (4), k_s was calculated to be 0.42 s^{-1} .

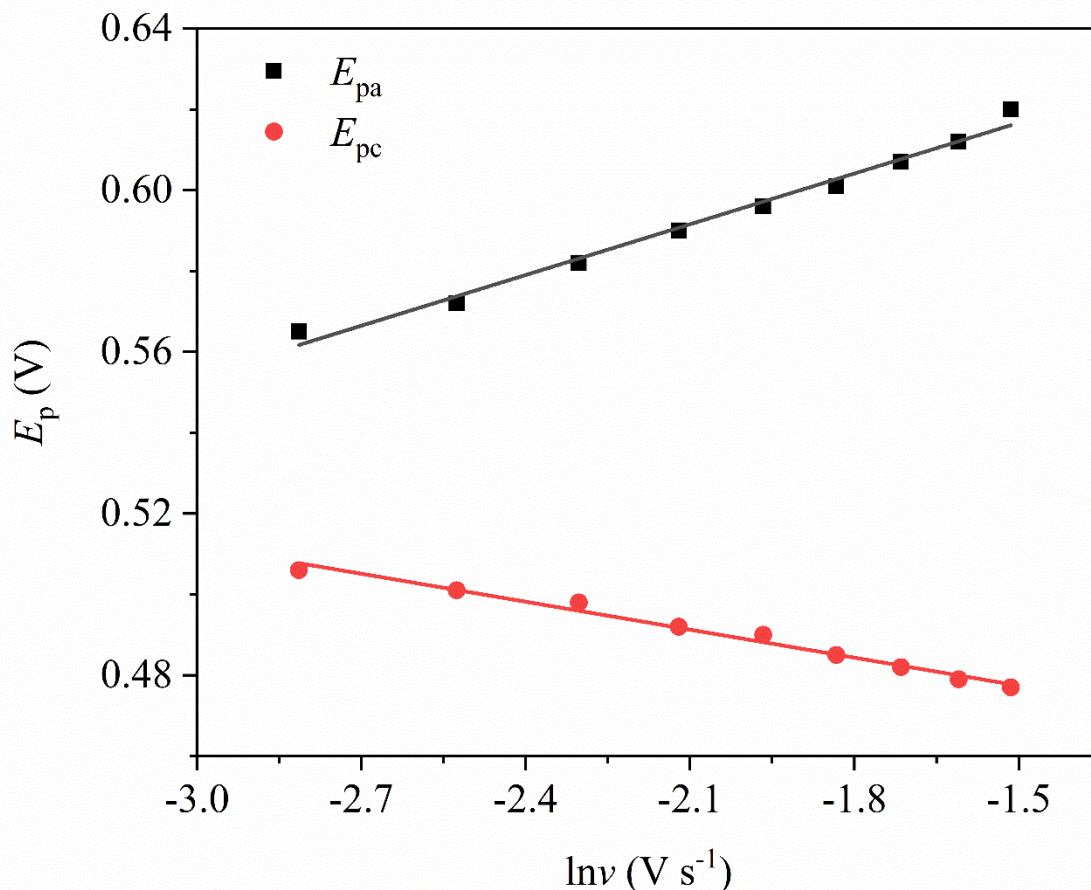


Figure 5. Relationship between the peak potential and $\ln v$.

3.4 Chronocoulometric studies

The saturated adsorption capacity (Γ^*) and diffusion coefficient (D) of DAPH on the Nafion/RGO-TEPA/GCE surface were calculated by the chronocoulometry curves of Nafion/RGO-TEPA/GCE in a 0.1 M PBS (pH = 2.2) solution in the absence (Fig. 6A, curve a) and presence (Fig. 6A, curve b) of DAPH (10 μM).

The corresponding Q - $t^{1/2}$ plots are provided in Fig. 6B, and the linear relationship of Q - $t^{1/2}$ corresponded to the following equations: $Q \text{ (}\mu\text{C)} = -55.44t^{1/2} - 156.42$ ($R^2 = 0.9995$) and $Q \text{ (}\mu\text{C)} = -87.15t^{1/2} - 314.25$ ($R^2 = 0.9978$). According to the Anson equation (equation (1) provided in Sec. 3.1), the value of Q_{ads} was calculated to be $1.47 \times 10^{-4} \text{ C}$ for the oxidation of adsorbed daphnetin, and D was $4.0 \times 10^{-8} \text{ cm}^2 \cdot \text{s}^{-1}$. The Γ^* of DAPH on Nafion/RGO-TEPA/GCE could be determined to be $3.79 \times 10^{-9} \text{ mol} \cdot \text{cm}^{-2}$ using Laviron's theory (5)

$$Q_{\text{ads}} = nFA\Gamma^* \quad (5)$$

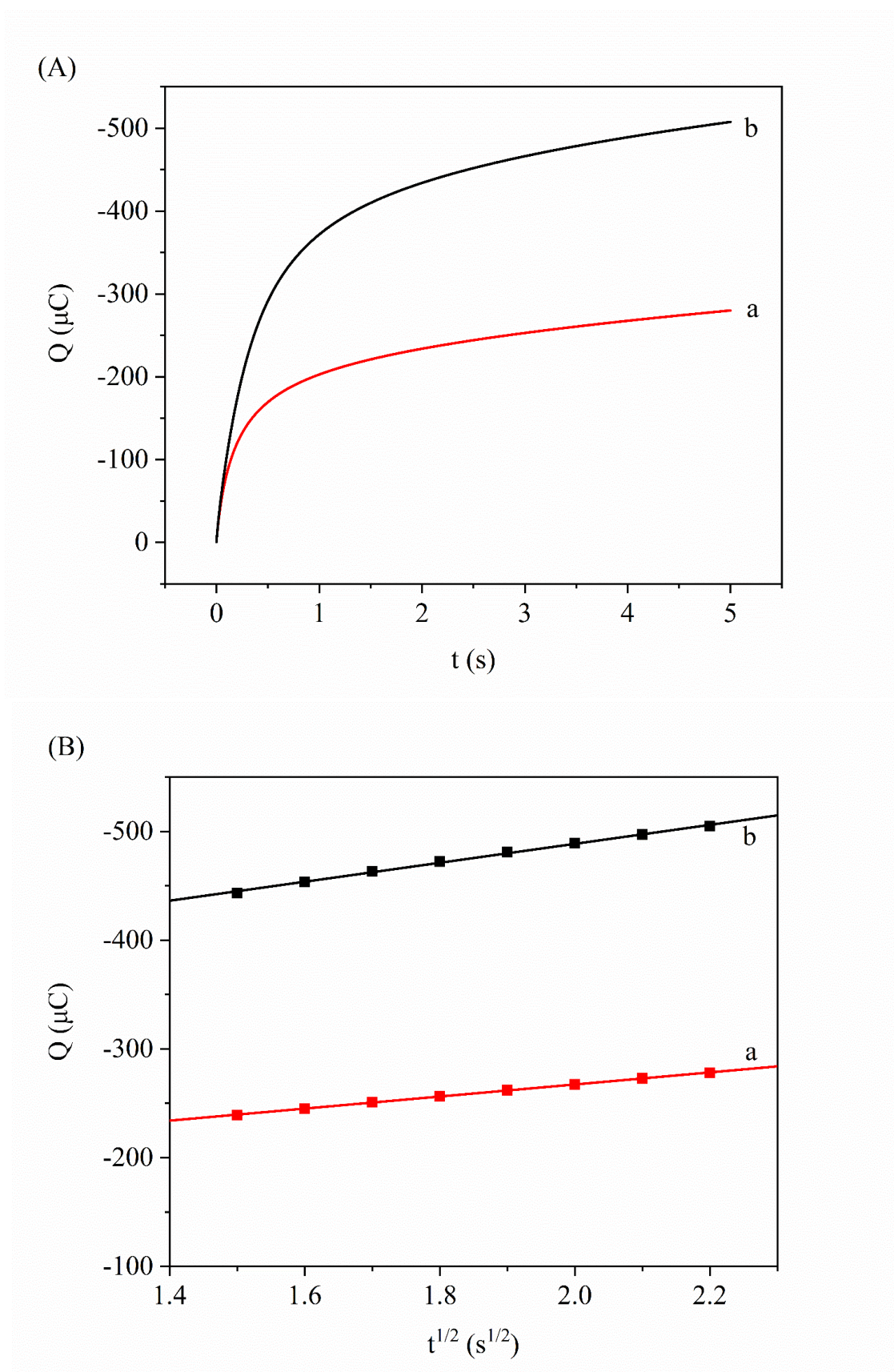


Figure 6. (A) Chronocoulometric curves of the background (curve a) and 10 μM DAPH in 0.1 M PBS (pH 2.2) on Nafion/RGO-TEPA/GCE (b). (B) Corresponding $Q-t^{1/2}$ plots.

3.5 Optimization of measurement parameters

3.5.1 Effect of pH

The redox peak current of DAPH was also greatly influenced by the pH value of the supporting electrolyte.

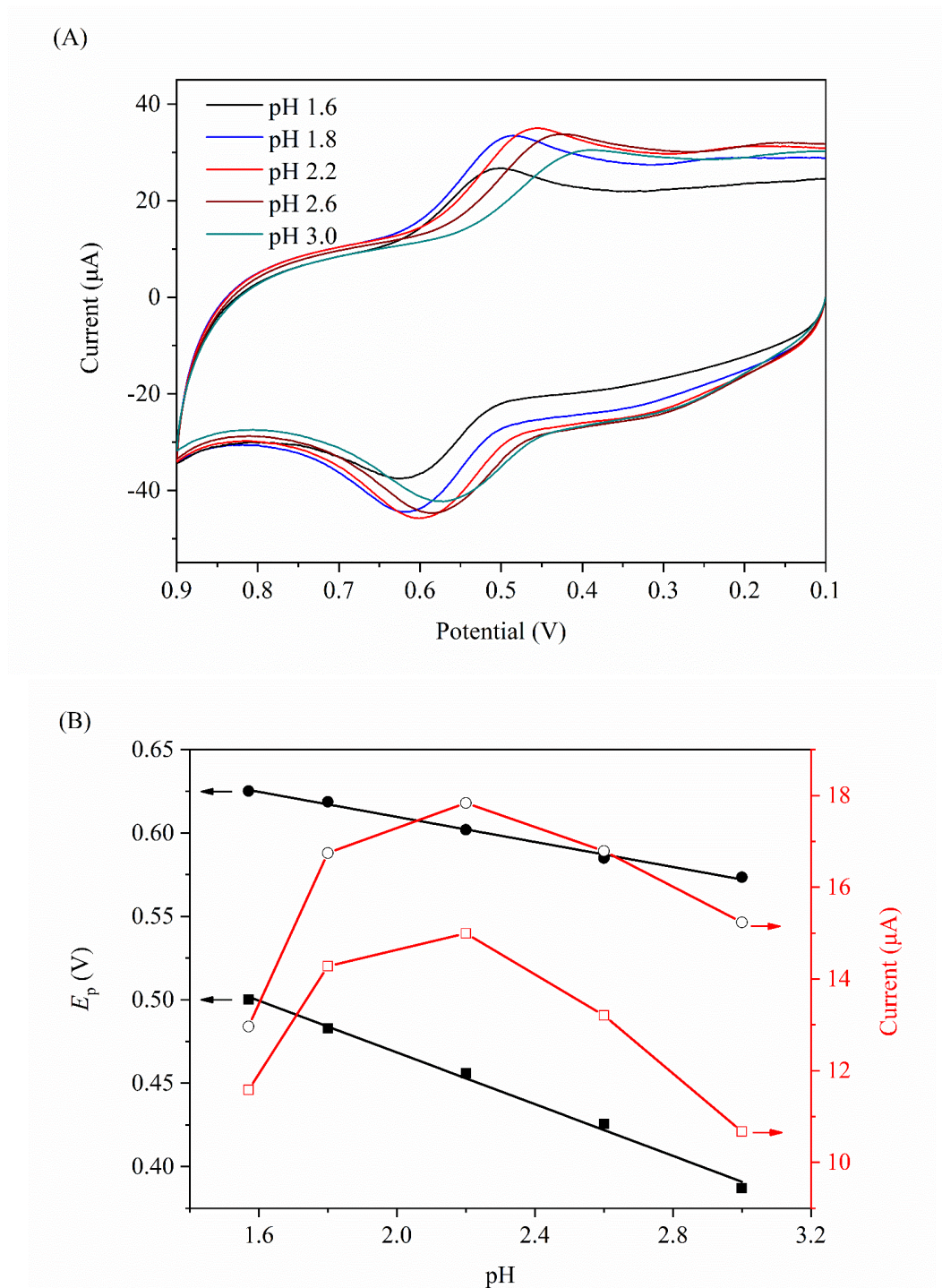


Figure 7. (A) CV curves of DAPH (10 μM) on Nafion/RGO-TEPA/GCE in 0.1 M PBS at different pH values (1.6, 1.8, 2.2, 2.6, 3.0) and a scan rate of 50 mV·s⁻¹. (B) pH-dependence of E_p and I .

Thus, the electrochemical response of DAPH (10 μM) on Nafion/RGO-TEPA/GCE was investigated by CV in PBS over a pH range of 1.6 ~ 3.0. As shown in Fig. 7A, the current intensity of DAPH first increased with an increasing pH value from 1.6 to 2.2, while continually increasing the pH value led to a decrease in the current intensity. Therefore, considering the detection sensitivity, a pH of 2.2 was chosen for further experiments.

From Fig. 7B, it is distinctly found that the redox peak potential of DAPH shifted negatively with an increasing pH, which means that protons are involved in the electrode reaction. The oxidation peak potential (E_{pa}) followed the linear equation $E_{\text{pa}} (\text{V}) = 0.685 - 0.0375 \text{ pH}$ ($R^2 = 0.9935$). The reduction peak potential (E_{pc}) followed the linear equation $E_{\text{pc}} (\text{V}) = 0.624 - 0.0776 \text{ pH}$ ($R^2 = 0.9929$). The slope value ($-37.5 \text{ mV}\cdot\text{pH}^{-1}$) was less than the theoretical value ($-59.0 \text{ mV}\cdot\text{pH}^{-1}$), suggesting the involvement of an unequal number of protons and electrons. According to the Nernst equation, the transferred number of electrons in the oxidation process was double the number of protons. According to the above results, it appeared that two electrons and one proton were involved in the redox reaction of daphnetin. This result is different from the reported references, where equal numbers of electrons and protons are involved in the redox reaction of daphnetin [9-11]. However, a similar result has also been reported in other references about Nafion-covered electrodes [26-29]. The possible reason might be due to the competition between DAPH and the proton with the Nafion film. [28].

3.5.2 Effect of the amount of RGO-TEPA on the oxidation peaks of DAPH

The amount of RGO-TEPA can directly change the properties and functions of the electrode surface and finally affect the detection of DAPH. Thus, the effect of the amount of RGO-TEPA was investigated by covering the GCE surface with 4 ~ 11 μL of RGO-TEPA solution. As shown in Fig. 8, the oxidation peak current increased with an increasing amount of RGO-TEPA up to 8 μL and then decreased gradually. This result should be attributed to the decreased electron-transfer rate resulting from the considerable thickness of the nanofilm formed by an excessive amount of RGO-TEPA. Therefore, 8 μL of RGO-TEPA solution was selected as the optimal amount for the preparation of the modified electrode.

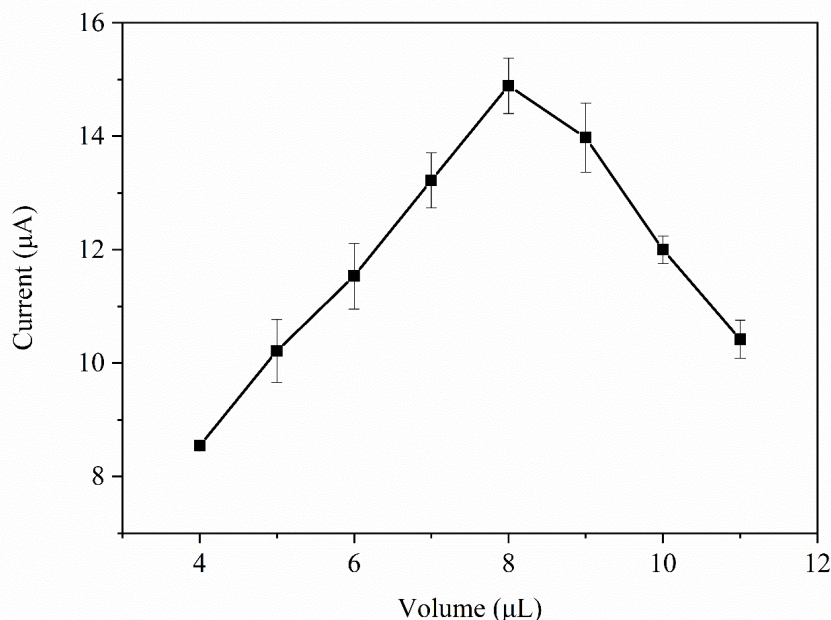


Figure 8. Effect of the accumulated volume of RGO-TEPA on the oxidation peak current of DAPH at a concentration of 1 mg mL^{-1} and a scan rate of $50 \text{ mV} \cdot \text{s}^{-1}$.

3.6 Analytical performance

3.6.1 Repeatability and reproducibility

The repeatability of Nafion/RGO-TEPA/GCE was evaluated by detecting the oxidation peak current of $10 \text{ } \mu\text{M}$ DAPH of one modified electrode by DPV. The relative standard deviation (RSD) for seven independent measurements was 1.6%. The reproducibility of the proposed sensor was estimated by the oxidation peak current of $10 \text{ } \mu\text{M}$ DAPH of five parallel modified electrodes by DPV under the same conditions. The RSD of the current response was 4.8%, which indicated the good reproducibility of the sensor.

3.6.2 Calibration curve and detection limit

Fig. 9A shows the oxidation peak current of different concentrations of DAPH under the optimal DPV conditions using Nafion/RGO-TEPA/GCE. The peak current had a linear relationship with the concentration of DAPH in the range of $0.01 \sim 1.0 \text{ } \mu\text{M}$ and $1.0 \sim 10 \text{ } \mu\text{M}$ (Fig. 9B). The linear regression equation could be expressed as $I_{\text{pa1}} (\mu\text{A}) = 4.798C (\mu\text{M}) + 0.021$ ($R^2 = 0.9975$, $0.01 \sim 1.0 \text{ } \mu\text{M}$) with a sensitivity of $23.87 \text{ } \mu\text{A L } \mu\text{M}^{-1} \text{ cm}^{-2}$, and $I_{\text{pa2}} (\mu\text{A}) = 1.678C (\mu\text{M}) + 3.816$ ($R^2 = 0.9931$, $1.0 \sim 10 \text{ } \mu\text{M}$) with a sensitivity of $8.35 \text{ } \mu\text{A } \mu\text{M}^{-1} \text{ cm}^{-2}$. The oxidation of DAPH on the modified electrode exhibited a high sensitivity at low concentrations and a low sensitivity at high concentrations. The low sensitivity at high concentrations may be due to fewer active sites and the kinetic limitations for the oxidation of DAPH [30]. Furthermore, the detection limit was calculated to be 0.5 nM ($S/N = 3$). As shown in Table

1, comparing the performance of our Nafion/RGO-TEPA/GCE sensor with previously reported DAPH sensors, Nafion/RGO-TEPA/GCE had a wider linear range and lower detection limit.

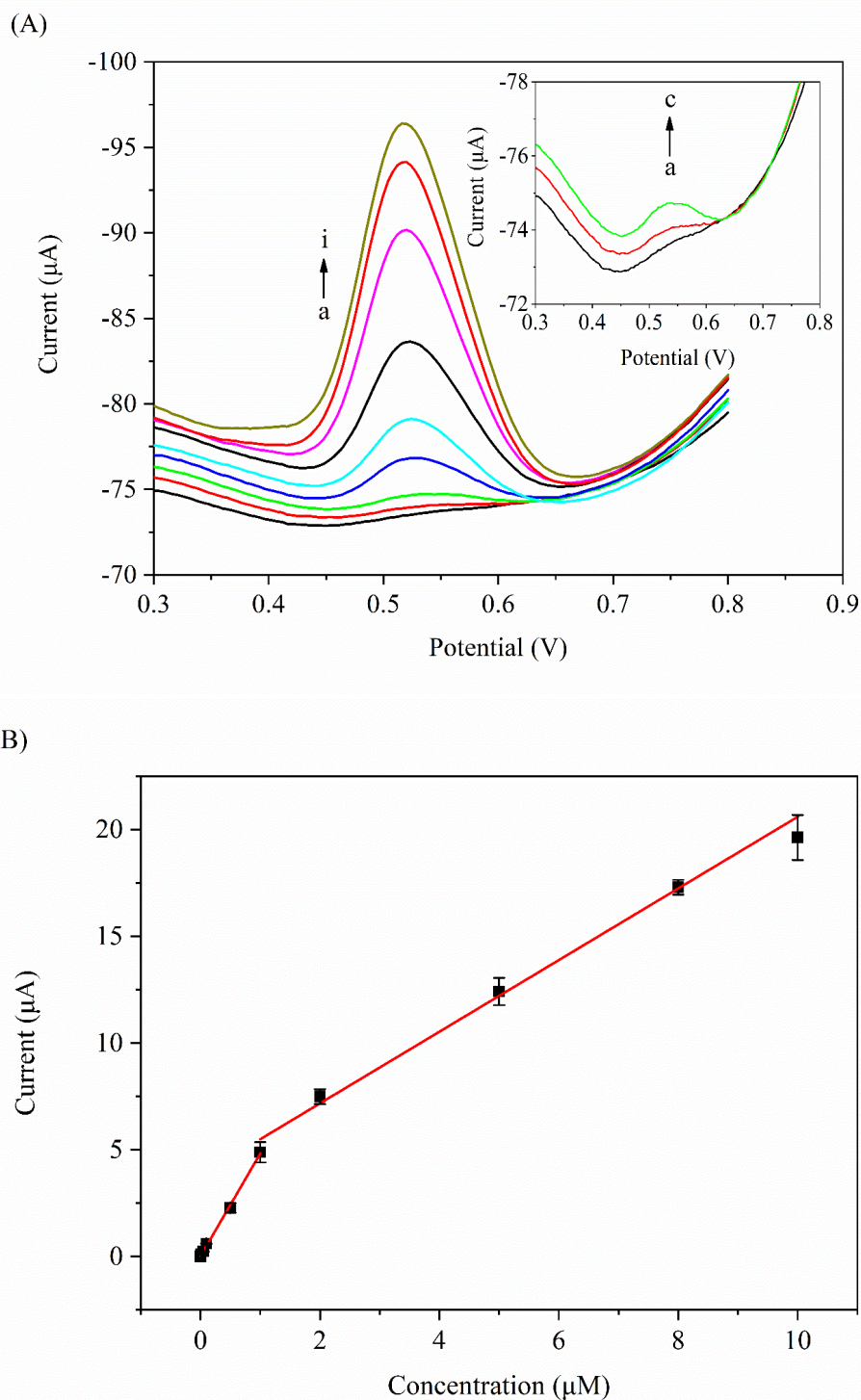


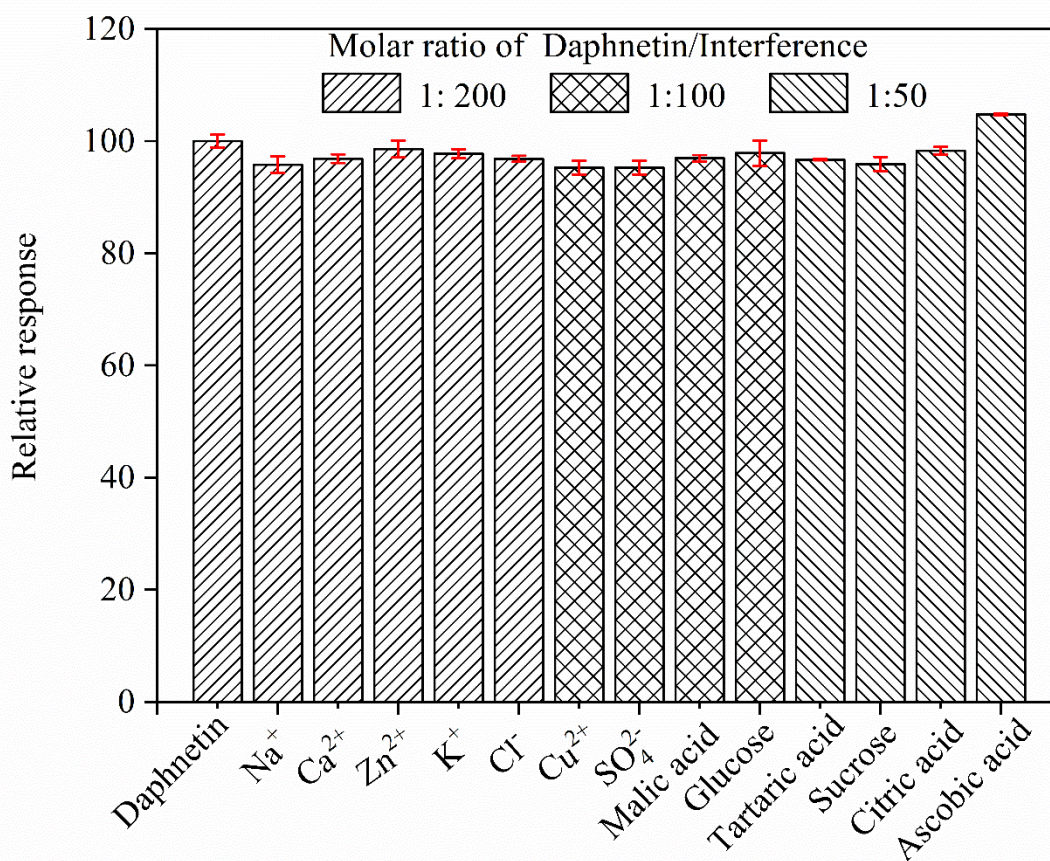
Figure 9. (A) DPV curves of DAPH on Nafion/RGO-TEPA/GCE in 0.1 M PBS (pH = 2.2) with different concentrations: (a) 0.01, (b) 0.05, (c) 0.1, (d) 0.5, (e) 1.0, (f) 2.0, (g) 5.0, (h) 8.0, and (i) 10.0 μM . The inset curve represents the DPV curves of Nafion/RGO-TEPA/GCE at low DAPH concentrations (a-c). (B) Calibration curve corresponding to the response of the modified sensor to the concentration of DAPH. Scan rate: $50 \text{ mV} \cdot \text{s}^{-1}$.

Table 1. Comparison of the electrochemical sensing performance of different modified electrodes toward DAPH detection.

Electrode	Linear range (μM)	LOD (nM)	Technique	Reference
ERGO/GCE	0.05~2	30	DPV	9
SDS-GN/SnO ₂ /GCE	0.03~8	8	DPV	10
Ca ₂ GeO ₄ -GR/GCE	0.02~0.9	6	DPV	11
Nafion/RGO-TEPA/GCE	0.01~10	0.5	DPV	This work

3.6.3 Interference studies

Under optimal experimental conditions, the potential interference from metal ions and organic compounds that may be present in pharmaceutical samples was investigated in a 10 μM DAPH solution by DPV. The tolerance limit was defined as the maximum concentration of the interfering species that caused an error of less than $\pm 5\%$. As shown in Fig. 10 (relative to the DAPH concentration), 200-fold concentrations of Na⁺, Ca²⁺, Zn²⁺, K⁺, and Cl⁻, 100-fold concentrations of Cu²⁺, SO₄²⁻, malic acid, glucose, and tartaric acid, 50-fold concentrations of sucrose, citric acid and ascorbic acid showed no interference on the detection of DAPH. These results indicated that the Nafion/RGO-TEPA/GCE sensor has an excellent anti-interference ability.

**Figure 10.** Relative analytical response ($I_{\text{Interference}}/I_{\text{DAPH}}$) of 10 μM DAPH in the presence of different interferents.

3.6.4 Real sample analysis

To verify the validity of the present method, it was employed to determine DAPH in Zushima tablets. The sample preparation procedure is described in Section 2.4. Briefly, 4.44 μL of the real sample solution was diluted to 25.00 mL by the supporting electrolyte and analyzed. A recognizable oxidation peak was observed for DAPH in the real sample. To evaluate the accuracy of the proposed method, the recovery test was also carried out by adding known levels of DAPH to the sample. Moreover, the sample was also detected by the HPLC method to further verify the accuracy of the proposed method. The obtained results are listed in Table 2. The recoveries of DAPH on Nafion/RGO-TEPA/GCE ranged from 101.5% to 108.5%, and the contents of DAPH detected by HPLC and the Nafion/RGO-TEPA/GCE sensor were in good agreement. From these excellent results, Nafion/RGO-TEPA/GCE was confirmed as an efficient electrode for the effective and accurate detection of DAPH in real samples.

Table 2. Recovery results for DAPH in Zushima tablet samples ($n = 3$)

Sample	DPV					HPLC	
	Added (μM)	Expected (μM)	Found (μM)	RSD (%)	Recovery (%)	Content in each tablet ($\text{mg}\cdot\text{tablet}^{-1}$)	Content in each tablet ($\text{mg}\cdot\text{tablet}^{-1}$)
Zushima tablets	0.000	0.000	0.197	4.8	-	5.03	5.12
	0.200	0.397	0.404	1.3	103.5		
	0.400	0.597	0.631	2.5	108.5		
	0.600	0.797	0.806	1.5	101.5		

4. CONCLUSIONS

In summary, a novel, reliable and sensitive sensor for the electrochemical detection of DAPH was successfully developed based on RGO-TEPA and Nafion through the dropwise addition of layers method. The sensor was first applied to detect DAPH in Zushima tablets. Under optimal conditions, a wide linear range (0.01 ~ 10.0 μM) with a detection limit of 0.05 nM, good reproducibility, and good selectivity were achieved on the Nafion/RGO-TEPA/GCE sensor due to the good electroconductivity and excellent electron transfer capability of RGO-TEPA. These results demonstrated better performance than the reported results for other DAPH-detecting sensors. The proposed sensing strategy may be potentially applied in the detection of other pharmaceuticals.

ACKNOWLEDGMENTS

The authors greatly acknowledge the financial support from Opening Project of Zhejiang Provincial First-rate Subject (Chinese Traditional Medicine), Zhejiang Chinese Medical University (No. Ya2017009).

References

1. F. G. Medina, J. G. Marrero, M. Macias-Alonso, M. C. Gonzalez, I. Cordova-Guerrero, A. G. Teissier Garcia and S. Osegueda-Robles, *Nat. Prod. Rep.*, 32 (2015) 1472.
2. G. Du, H. Tu, X. Li, A. Pei, J. Chen, Z. Miao, J. Li, C. Wang, H. Xie, X. Xu and H. Zhao, *Neurochem. Res.*, 39 (2014) 269.
3. G. J. Finn, B. S. Creaven and D. A. Egan, *Biochem. Pharmacol.*, 67 (2004) 1779.
4. K. C. Fylaktakidou, D. J. Hadjipavlou-Litina, K. E. Litinasc and D. N. Nicolaidis, *Curr. Pharm. Des.*, 10 (2004), 3813.
5. Q. Gao, J. Shan, H. Xu, X. Cai, H. Tong and L. Jiang, *Chin. J. New Drugs*, 16 (2007) 2021.
6. Q. Gao, J. J. Shan, L. Q. Di, L. J. Jiang and H. Q. Xu, *J. Ethnopharmacol.*, 120 (2008) 259.
7. D. A. Egan, C. Duff, L. Jordan, R. Fitzgerald, S. Connolly and G. Finn, *Chromatographia*, 58 (2003) 649.
8. J. Chen, X. Liu and Y. P. Shi, *Anal. Chim. Acta.*, 523 (2004) 29.
9. W. Qiao, Y. Li, L. Wang, G. Li, J. Li and B. Ye, *J. Electroanal. Chem.*, 74 (2015) 68.
10. S. Jing, H. Zheng, L. Zhao, L. Qu and L. Yu, *J. Electroanal. Chem.*, 787 (2017) 72.
11. Y. Fu, L. Wang, D. Huang, L. Zou and B. Ye, *J. Electroanal. Chem.*, 801 (2017) 77.
12. G. Darabdhara, M. R. Das, S. P. Singh, A. K. Rengan, S. Szunerits and R. Boukherroub, *Adv. Colloid Interface.*, 217 (2019) 101991.
13. S. J. Rowley-Neale, E. P. Randviir, A. S. Abo Dena and C. E. Banks, *Appl. Mater. Today*, 10 (2018) 218.
14. W. Mao, J. He, Z. Tang, C. Zhang, J. Chen, J. Li and C. Yu, *Biosens. Bioelectron.*, 131 (2019) 67.
15. J. Chen, C. Yu, Y. Zhao, Y. Niu, L. Zhang, Y. Yu, J. Wu and J. He, *Biosens. Bioelectron.*, 91 (2017) 892.
16. H. Zhong, C. Yu, R. Gao, J. Chen, Y. Yu, Y. Geng, Y. Wen and J. He, *Biosens. Bioelectron.*, 144 (2019) 111635.
17. H. Ma, X. Zhang, X. Li, R. Li, B. Du and Q. Wei, *Talanta*, 143 (2015) 77.
18. S. Zhao, Y. Zhang, S. Ding, J. Fan, Z. Luo, K. Liu, Q. Shi, W. Liu and G. Zang, *J. Electroanal. Chem.*, 834 (2019) 33.
19. X. Zhang, F. Li, Q. Wei, B. Du, D. Wu and H. Li, *Sensor. Actuat. B-Chem.*, 194 (2014) 64.
20. S. Yu, G. Zou and Q. Wei, *Talanta*, 156-157 (2016) 11.
21. L. Cao, C. Fang, R. Zeng, X. Zhao, F. Zhao, Y. Jiang and Z. Chen, *Sensor. Actuat. B-Chem.*, 252 (2017) 44.
22. D. Wu, A. Guo, Z. Guo, L. Xie, Q. We and B. Du, *Biosens. Bioelectron.*, 54 (2014) 634.
23. F. C. Anson, *Anal. Chem.*, 38 (1966) 54.
24. H. Zhang, Y. Shang, T. Zhang, K. Zhuo and J. Wang, *Sensor. Actuat. B-Chem.*, 242 (2017) 492.
25. E. Laviron, *J. Electroanal. Chem.*, 101 (1979) 19.
26. E. Mynttinen, N. Wester, T. Lilius, E. Kalso, J. Koskinen and T. Laurila, *Electrochim. Acta*, 295 (2019) 347.
27. J. Liu, W. Weng, C. Yin, G. Luo, H. Xie, Y. Niu, X. Li, G. Li, Y. Xi, Y. Gong, S. Zhang and W. Sun, *Int. J. Electrochem. Sci.*, 14 (2019) 1310.
28. Y. Wang, H. Ge, G. Ye, H. Chen and X. Hu, *J. Mater. Chem. B*, 3 (2015) 3747.
29. C. Montes, A. M. Contento, M. J. Villaseñor and Á. Ríos, *Microchimica Acta*, 187 (2020) 190.
30. R. Nehru, Y. F. Hsu and S. F. Wang, *Anal. Chim. Acta*, 1122 (2020) 76.